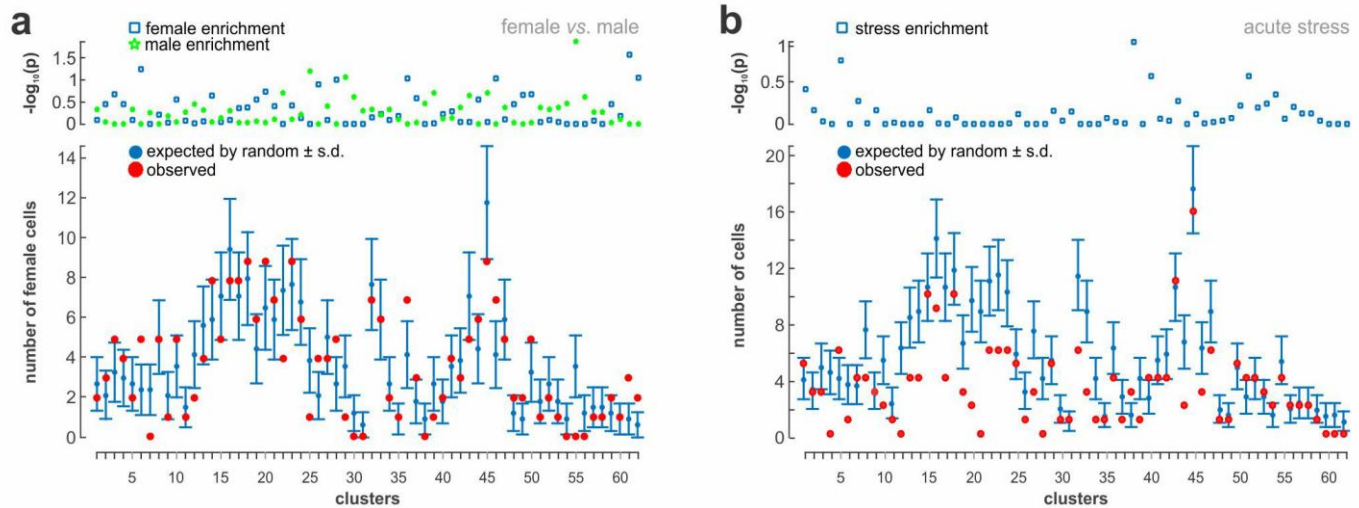


## Supplementary Figure 1

### Methodological considerations for and quality control of single-cell RNA-seq

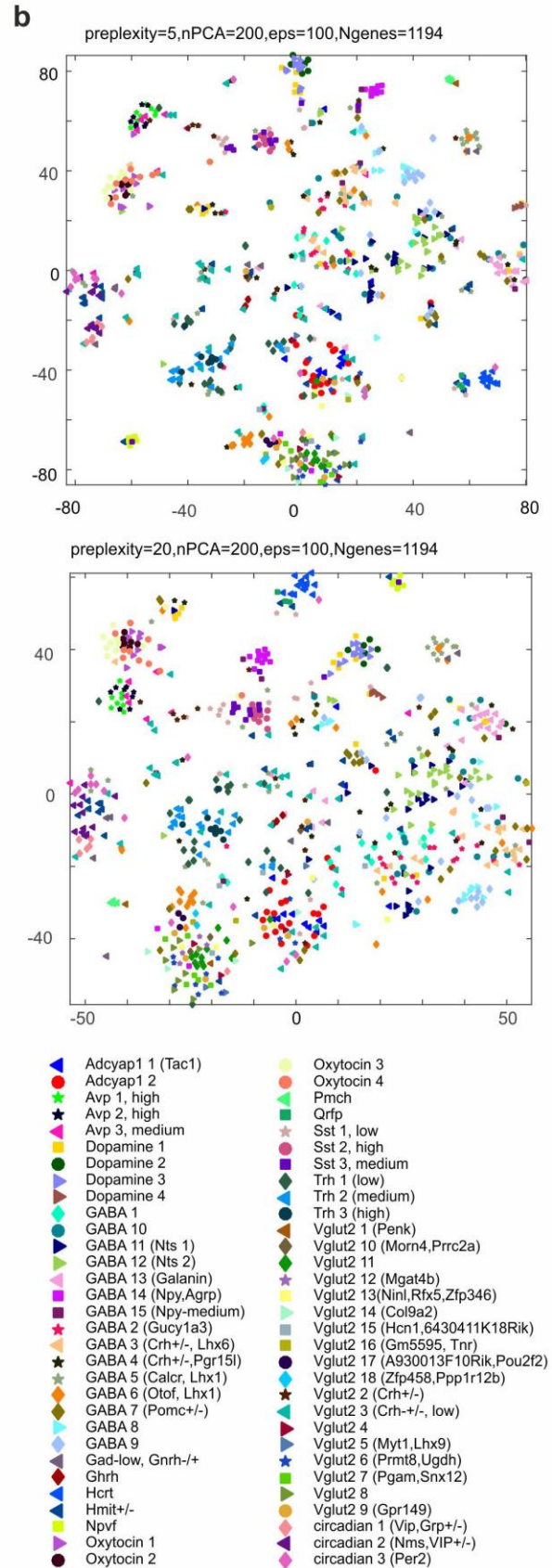
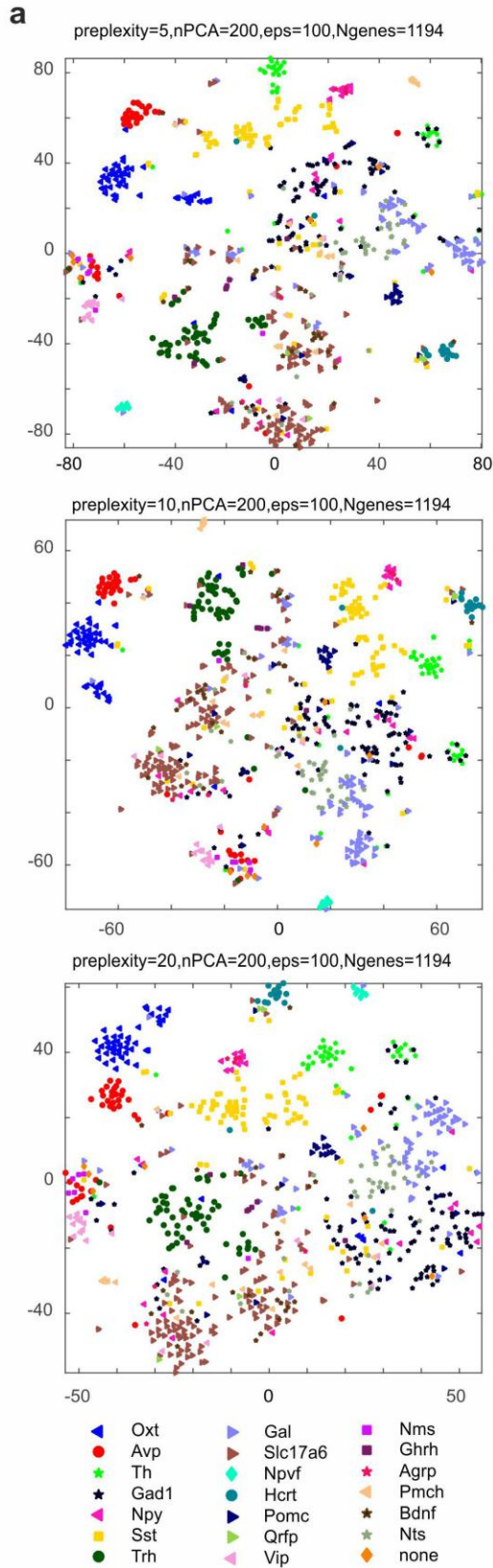
(**a**) Neuron numbers per cluster in our analysis (*blue boxes*), and comparison of actual numbers in repeat experiments with statistical probing of random distribution (*solid red circles*). Note that this comparison excluded sampling or processing-related bias due either to false positive observations or undersampling. (**b**) Bar plots show the total number of genes detected in individual neuronal subtypes. (**c**) Likewise, the total number of mRNA molecules passing our filtering criteria (see *Online Methods*) were plotted. Grey circles and error bars represent means  $\pm$  s.e.m. per group in (**b,c**).



## Supplementary Figure 2

### Sex and acute stress do not bias neuronal clustering

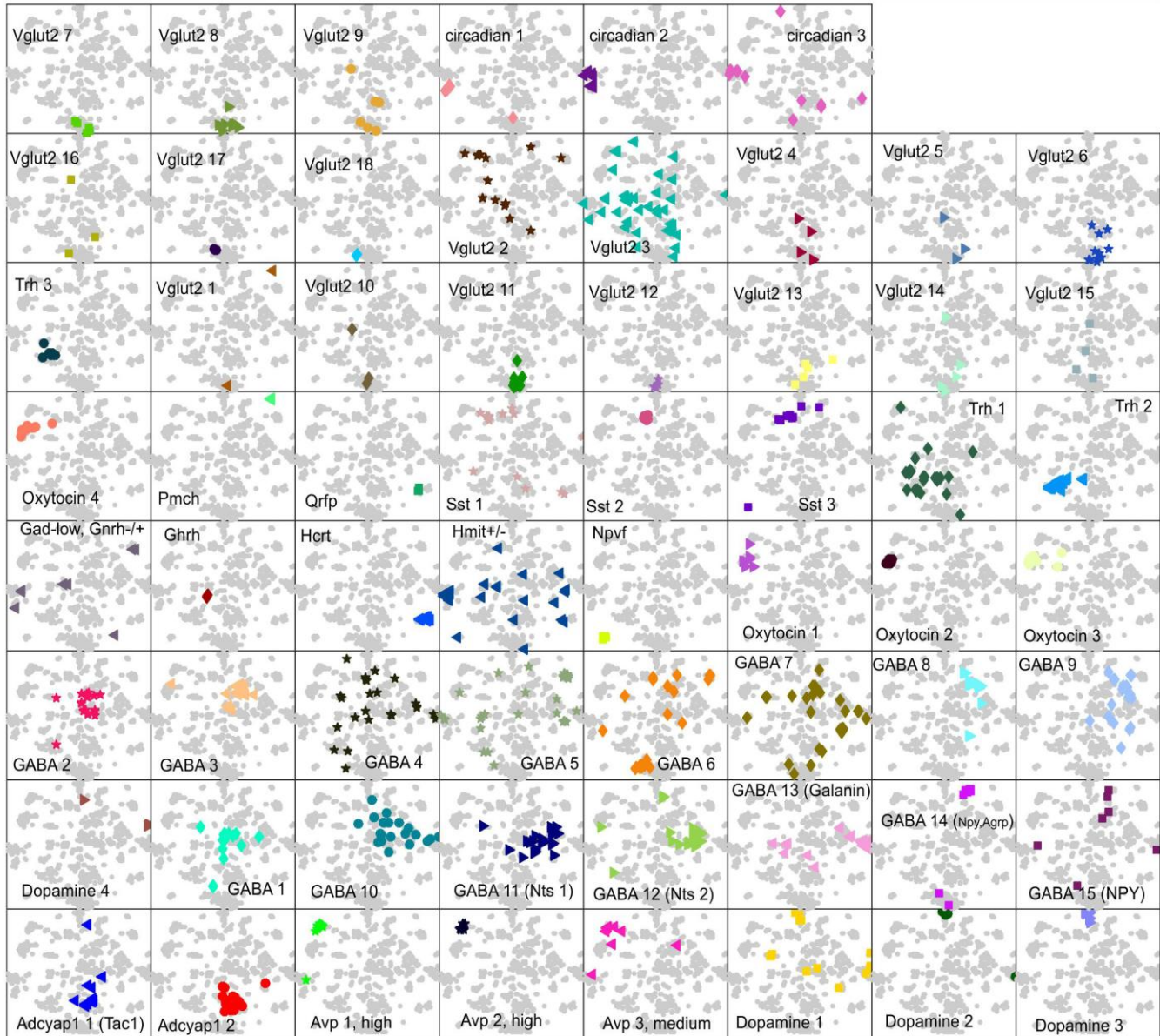
(a) Numbers of cells from female animals in each cluster ('observed') with respect to the range expected by random sampling ('expected by random  $\pm$  s.d.'). Clusters on the ordinate follow their listing in *Figure 2*. The overall frequency of cells of female origin was 30% in the neuronal dataset. The expected means  $\pm$  s.d. were calculated from the binomial distribution ( $\text{Bin}(N,p)$  where  $p = 0.3$  and  $N =$  the number of cells in each cluster). Clusters show no significant bias for sampling. Clusters #6 and #55 lean towards female and male dominance, respectively. Note that cluster #7 only contains neurons from males. *Upper panel*:  $p$  values calculated using binomial distribution for enrichment of males/females in each cluster. (b) Cluster distribution of cells isolated from animals 6h after acute formalin stress. Solid red circles denote neurons from stress-exposed animals ('observed'). Blue bars represent the binomial distribution as calculated if distribution was random ('expected by random  $\pm$  s.d.'). *Upper panel*:  $p$  values calculated using binomial distribution for enrichment of cells from stress-exposed animals in each cluster. None of the clusters showed stress-related bias.



### Supplementary Figure 3

#### Visualization of hypothalamic neuron subtypes on two-dimensional maps using tSNE

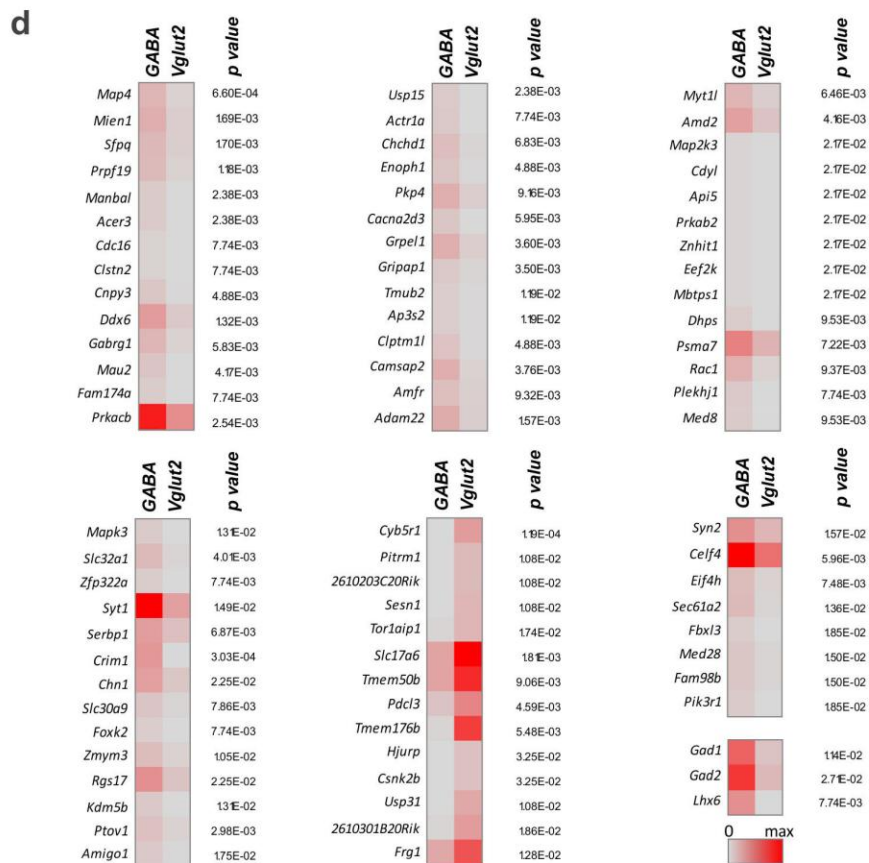
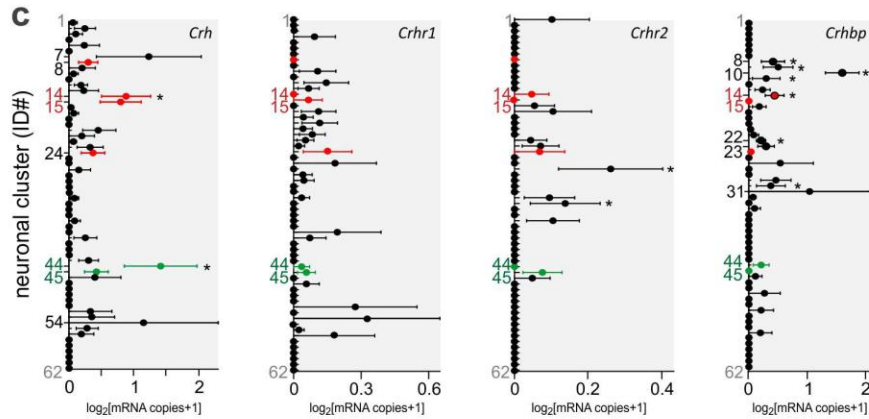
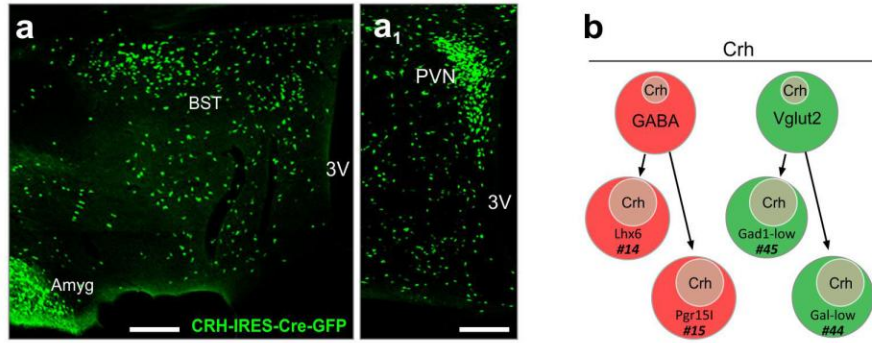
1,194 genes, perplexity = 5, 10 or 20 with 200 principle components. Neurons were color-coded by highest expression of well-known, cluster-defining hypothalamic markers. **(a)** Distribution of neurons expressing select neuropeptide and neurotransmission-related genes. **(b)** Distribution of 62 neuronal clusters determined by the BackSpinV2 algorithm. For abbreviations we refer to *Figures 1* and *2* of the manuscript.



**Supplementary Figure 4**

**Distribution of 62 neuronal clusters determined by the BackSpinV2 algorithm**

Data for each cluster is shown separately on a cumulative tSNE background. Please note that most of the 62 groups are clustered in terms of tSNE plot coordinates while some show lower stringency: 46 of 62 clusters as relatively well separated in the tSNE plot with forming visual clusters with or without outliers; 10 neuronal groups as “satisfactory” clustered with more than one separation core or by forming segregated groups with a relatively large distance between individual neurons. Several clusters do not form segregated groups in tSNE plots: *Vglut2* 1, *Vglut2* 3, *Vglut2* 16, *Hmit*<sup>+/-</sup>, GABA 4, GABA 5 because of several possible reasons: a deeper inner heterogeneity of the clusters *Vglut2* (all), *Hmit*<sup>+/-</sup> and GABA 5, their mixed phenotypes and/or a low number of genes segregating those cells. One needs to remember fundamental algorithmic differences between BackSpin and tSNE: BackSpin can “ignore” genes (which are enriched in other clusters) when splitting the current group. In contrast, tSNE always considers all genes. Thus, tSNE will be more sensitive to carryover of mRNA and contamination by doublets than BackSpin. Individual data points correspond to single cells.



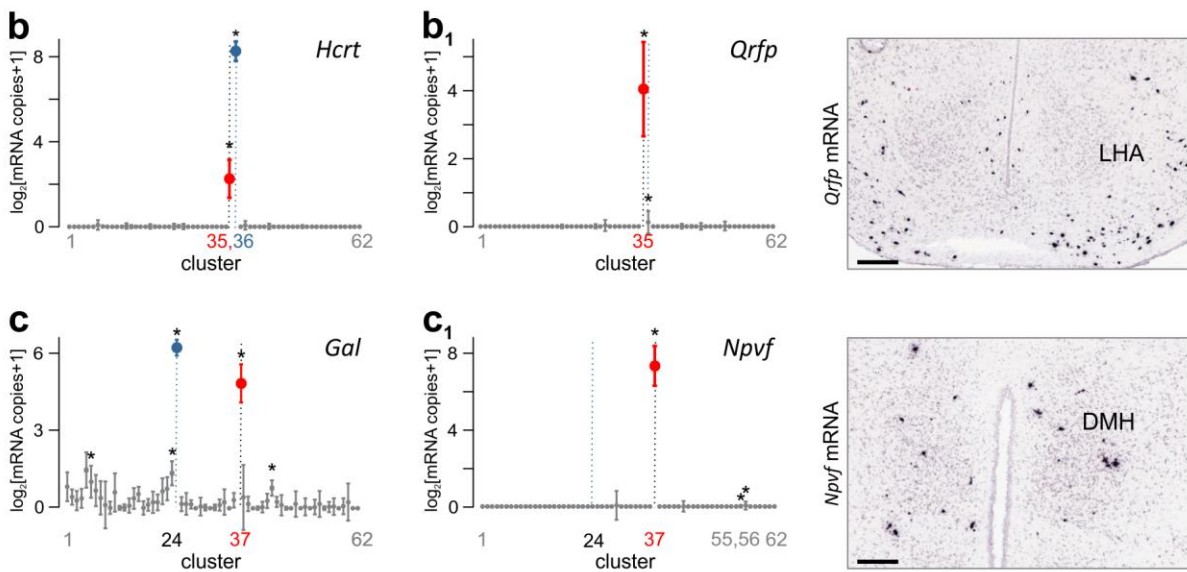
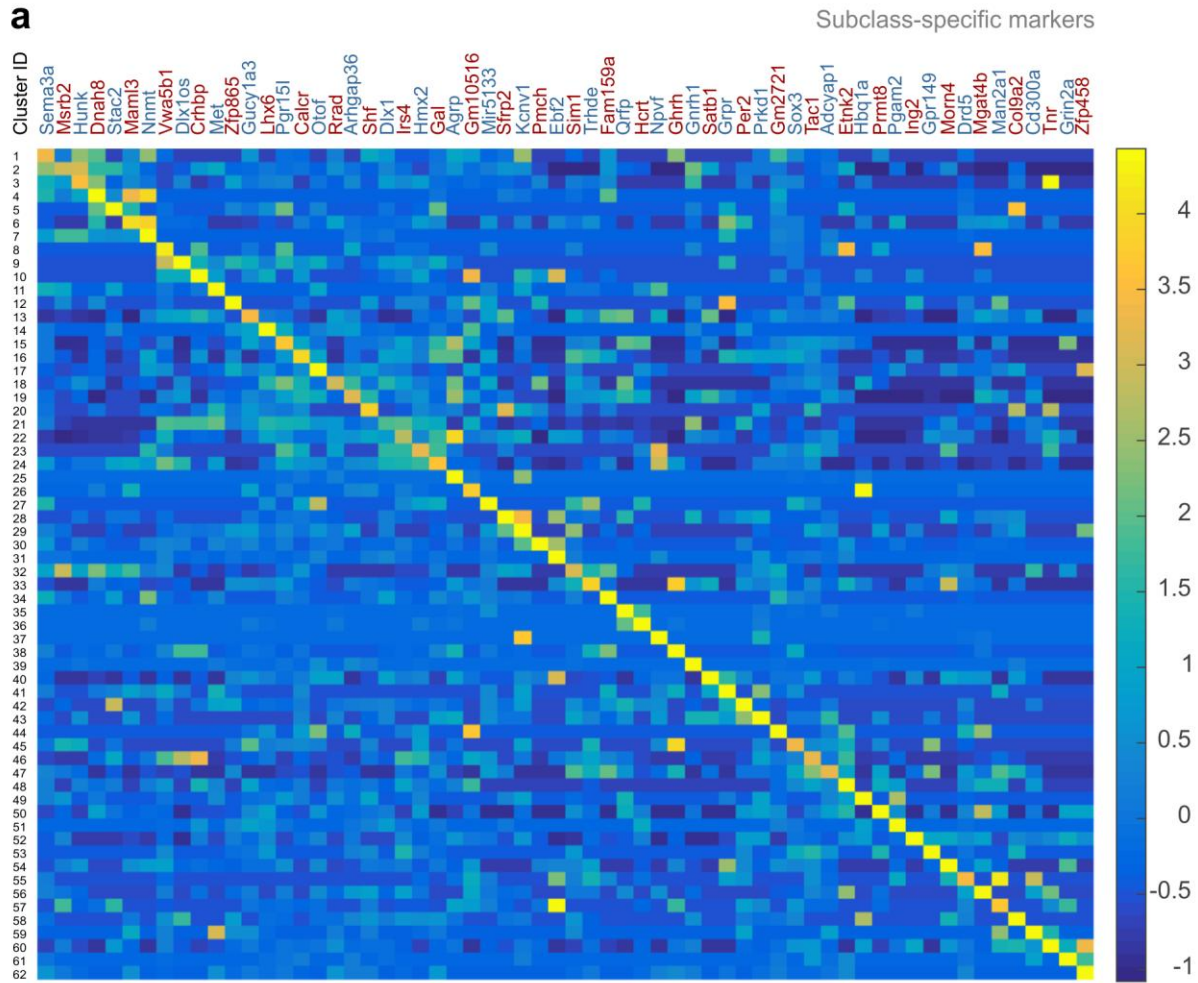
## Supplementary Figure 5

### Heterogeneity of corticotropin-releasing hormone systems in the mouse hypothalamus

(**a, a<sub>1</sub>**) Genetic tracing reveals the distribution of *Crh*<sup>+</sup> neurons concentrated in the bed nucleus of stria terminalis (BST, **a**)<sup>1-3</sup> and paraventricular hypothalamic nucleus (PVH, **a<sub>1</sub>**), as well as shows scattered neurons with a history of *Crh* expression<sup>4,5</sup>. (**b**) Taxonomy of *Crh*<sup>+</sup> neurons in the mouse hypothalamus. Note that dual GABA/glutamate phenotypes exist. Cluster numbers are as per *Figure 2*. (**c**) *Crh*, CRH receptors 1,2 (encoded by *Crhr1/2* genes) and CRH-binding protein (*Crhbp* gene) mRNA expression in hypothalamic neuronal subtypes (vertical axes). Expression levels (horizontal axis) were plotted as means of  $\log \pm$  s.e.m. Red and green colors identify GABAergic and glutamatergic clusters (#44 and #45), which express *Crh* mRNA at levels exceeding 2x s.e.m. Note that significant levels of gene expression in clusters were found only for *Crhr2* and *Crhbp* but not for *Crhr1* (\* $q < 0.05$ ). *Crhr1* and *Crhr2* were mostly present at low copy numbers in sparse hypothalamic neurons amongst different subtypes. (**d**) Heat-map representation of genes differentially expressed between GABAergic and glutamatergic *Crh*<sup>+</sup> neurons. Increasing color intensity towards red is proportionate to higher mRNA content. Only  $p$  values (Wilcoxon rank-sum test) are shown yet all  $q$  values were also  $< 0.05$ ;  $n = 10$  (GABA) and  $n = 11$  (glutamate) neurons in discrete branches of taxonomy. In GABA<sup>+</sup>/*Crh*<sup>+</sup> neurons, we observed a predominance of *Prkacb* (encoding c-AMP-dependent protein kinase subunit B), *Amd2* (coding for S-adenosylmethionine decarboxylase 2), *Psm7* (encoding proteasome subunit  $\alpha 7$ ), *Syt1* (encoding synaptotagmin 1), *Crim1* (producing cysteine rich transmembrane BMP regulator 1), *Chn1* (coding for chimerin 1), *Rgs17* (encoding regulator of G protein signaling 17), *Syn2* (producing synapsin 2), *Celf2* (coding for Elav-like family member 2) and *Sec61a2* (encoding translocon  $\alpha 2$  subunit). Glutamatergic neurons were found to express higher levels of *Tmem50b* (that is, transmembrane protein 50B protein), *Tmem176b* (encoding transmembrane protein 176B), *Pdcl3* (coding for phosphocin-like protein 3), *Usp31* (encoding ubiquitin-specific peptidase 31), *Frg1* (encoding FSHD region gene 1) and *Cyb5r1* (producing cytochrome b5 reductase 1). Scale bars = 250  $\mu$ m (**a, a<sub>1</sub>**). Abbreviation: 3V, third ventricle.

#### References:

1. Hrabovszky, E., Wittmann, G., Turi, G.F., Liposits, Z. & Fekete, C. Hypophysiotropic thyrotropin-releasing hormone and corticotropin-releasing hormone neurons of the rat contain vesicular glutamate transporter-2. *Endocrinology* **146**, 341-347 (2005).
2. Lee, Y. & Davis, M. Role of the hippocampus, the bed nucleus of the stria terminalis, and the amygdala in the excitatory effect of corticotropin-releasing hormone on the acoustic startle reflex. *J Neurosci.* **17**, 6434-6446 (1997).
3. McNally, G.P. & Akil, H. Role of corticotropin-releasing hormone in the amygdala and bed nucleus of the stria terminalis in the behavioral, pain modulatory, and endocrine consequences of opiate withdrawal. *Neuroscience* **112**, 605-617 (2002).
4. Palkovits, M. Stress-induced expression of co-localized neuropeptides in hypothalamic and amygdaloid neurons. *European journal of pharmacology* **405**, 161-166 (2000).
5. Watts, A.G., Sanchez-Watts, G. & Kelly, A.B. Distinct patterns of neuropeptide gene expression in the lateral hypothalamic area and arcuate nucleus are associated with dehydration-induced anorexia. *J Neurosci.* **19**, 6111-6121 (1999).

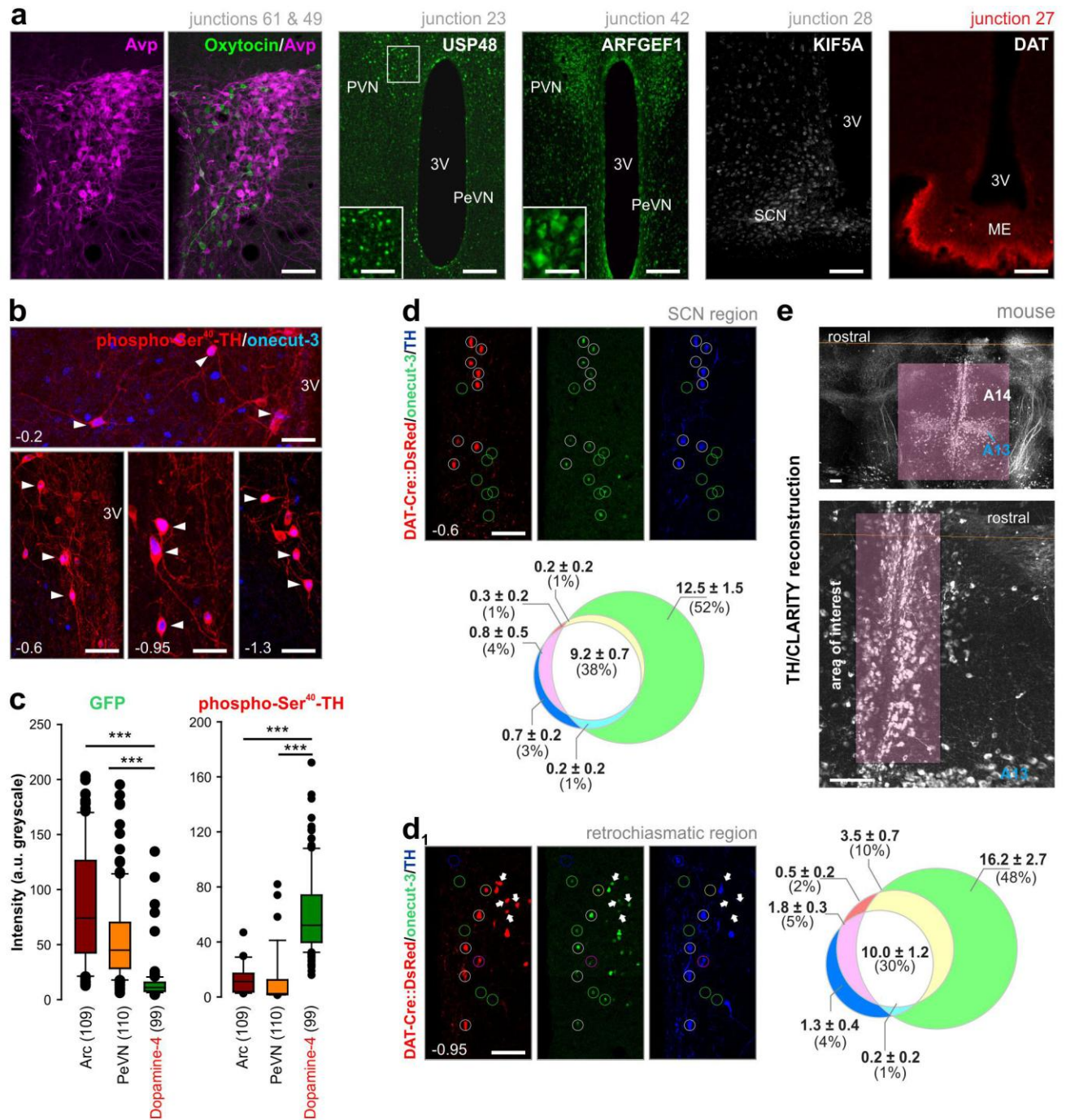


Supplementary Figure 6



## Representative markers for hypothalamic neuronal subtypes and their localization

(a) For each neuronal cluster, the most specific markers were calculated (gene names are on top). To identify the most unique markers for each neuronal cluster, we used  $power = 0$  analysis to identify topmost-expressed unique genes. To force uniqueness, we excluded genes that appear in the list of top 5 markers in other clusters. Since we often observed clusters that are characterized by gene combinations rather than unique global markers, some of the top 5 markers showed low specificity. All genes were found to be statistically significant by the Wilcoxon rank-sum test ( $q < 0.05$ ) with the exception of *L3hypdh* ( $p = 0.04$ ), *Prkd1* ( $p = 0.007$ ) and *Ing2* ( $p = 0.01$ ). The color scale to the right presents values after log transform, which were centered and normalized to mean = 0 and s.d. = 1 for each gene. Saturated colors represent the upper and lower 1% (range 1-99%). (b-c) Novel neuropeptide identities in the hypothalamus. Hypocretin (*Hcrt*, b) and galanin (*Gal*, c)-containing neuronal clusters (#35 and #37, respectively) uniquely co-express mRNAs for pyroglutamylated RFamide peptide (*Qrfp*; b<sub>1</sub>) and neuropeptide VF precursor (*Npvf*, c<sub>1</sub>). Note that *Hcrt*<sup>+</sup> cluster #36 lacks *Qrfp* expression. *In situ* hybridization identifies *Qrfp*<sup>+</sup> or *Npvf*<sup>+</sup> neurons in the arcuate nucleus (Arc)-lateral hypothalamic area (LHA) and dorsomedial hypothalamus (DMH), respectively. Histochemical data are from the Allen Brain Atlas ([www.brain-map.org](http://www.brain-map.org)). Scale bars = 150  $\mu$ m. mRNA copy numbers were expressed as means  $\pm$  s.e.m. ( $\log_2(\text{mRNA copies} + 1)$ ;  $power = 1$ ). \* $q < 0.05$  (Wilcoxon rank-sum test corrected for multiple testing).

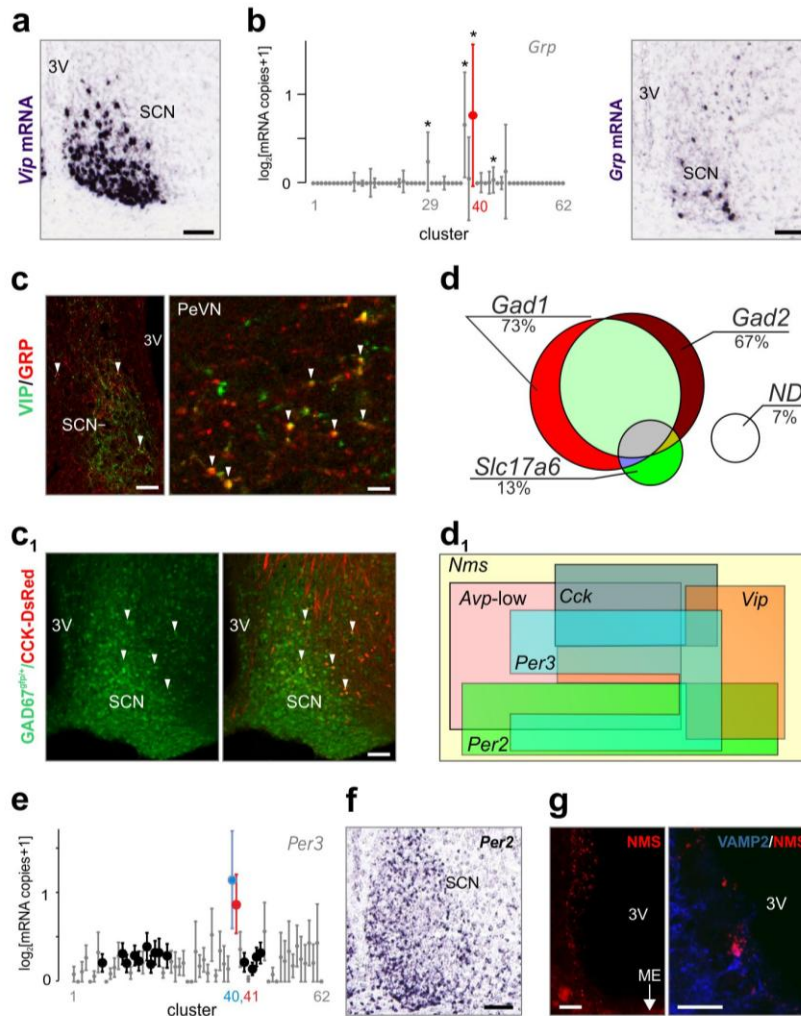


Supplementary Figure 7

### Histochemical analysis of novel neuronal markers and A14 neurons in the mouse hypothalamus

(a) Novel markers for hierarchical junctions in the hypothalamic diagram (Figure 2). From left to right: oxytocin and Arg-vasopressin (Avp) in the magnocellular paraventricular nucleus of the hypothalamus (PVN), ubiquitin-specific peptidase 48 (USP48), ADP-ribosylation factor guanine nucleotide-exchange factor 1 (AARFGEF1), kinesin family member 5A (KIF5A), as well as dopamine transporter (DAT) expression at the median eminence. (b) Morphology of A14 periventricular dopamine neurons across the mouse hypothalamus. Phosphorylated-TH and oncut-3 co-existence was taken as positive cell identification (arrowheads). Numbers denote anterior-posterior coordinates relative to Bregma. (c)

Quantitative immunofluorescence microscopy reveals an inverse relationship between the intensities of GFP and phospho-Ser<sup>40</sup>-TH (p-Ser<sup>40</sup>-TH) immunoreactivities for periventricular dopamine neurons in *Th*-GFP reporter mice. \*\*\* $p < 0.001$  between the groups indicated. Bracketed numbers denote group sizes. Data in box plots represent medians and 10<sup>th</sup>, 25<sup>th</sup>, 70<sup>th</sup> and 90<sup>th</sup> percentiles. (**d,d<sub>1</sub>**) Representative confocal micrographs of coronal single optical sections from the periventricular region of *Dat1*-tdTomato mice at select anterior-posterior subdivisions stained for onecut-3 and TH. Endogenous tdTomato signal was not amplified. Venn diagrams show the average number of *Dat1*-tdTomato (*red*), onecut-3 (*green*) and TH (*blue*) immunoreactive (ir) neurons  $\pm$  s.e.m. per optical slice ( $n = 6$  animals). The relative number of immunoreactive somata compared to the total number of cells is denoted as percentages. Overlap represents co-localization. Note the high degree of co-localization for the tdTomato signal with TH and onecut-3 immunoreactivities. Also note a cluster of tdTomato cells at the retrochiasmatic region that are onecut-3<sup>+</sup> but likely lack appreciable TH expression. All encircled cells in the photomicrographs were color-coded according to the cell's fluorescence labeling. Bregma levels were indicated at the bottom-left. (**e**) Single-plane views of CLARITY-reconstructed mouse hypothalami stained for TH and focusing on the A14 cell group (semi-transparent overlay). Images were taken at a semi-horizontal plane, with the lower focusing on A14 neurons (see also *Supplementary Movie 3*). *Abbreviations*: 3V, third ventricle; A13, zona incerta; Arc, arcuate nucleus; PeVN, periventricular nucleus; SCN, suprachiasmatic nucleus. *Scale bars* = 150  $\mu$ m (**a** [junctions 61/49, 23 *inset*, 28, 27]), 250  $\mu$ m (**a** [junction 23, 42], **e**), 50  $\mu$ m (**d,d<sub>1</sub>**), 45  $\mu$ m (**a** [junction 42 *inset*], **b**).



Supplementary Figure 8

### Neuronal heterogeneity in the suprachiasmatic nucleus

(a) *In situ* hybridization histochemistry showing the expression of vasoactive intestinal polypeptide (*Vip*) mRNA in the suprachiasmatic nucleus (SCN). (b) Likewise, gastrin-releasing peptide (*Grp*) mRNA was selectively detected in cluster #40 and histochemically localized to the SCN. (c) VIP/GRP co-existence in boutons within the SCN and terminals in the periventricular nucleus (PeVN). (c<sub>1</sub>) GABAergic neuronal components (green), including a subset of neurons and axonal pathways co-expressing (arrowheads) a DsRed construct under the control of the *Cck* promoter (blue) are shown in a dual-reporter mouse, highlighting the abundance of GABA neurons in the SCN. (d) *Top*: Neurotransmitter heterogeneity in the SCN. Overlapping parts of the Venn diagram denote dual GABA/glutamate neurons. ND: non-defined. *Bottom*: Molecular heterogeneity of neuromedin S-containing neurons. Note the abundance of clock genes, *Vip* and *Cck*. (e) Differential *Per3* mRNA expression in neuronal subclasses of the hypothalamus. Note highest levels of *Per3* mRNA assignment to clusters #40 and #41. Red color denotes expression levels of > 2x s.e.m. from zero. Clusters were ordered according to *Figure 2*. mRNA copy numbers were expressed as means  $\pm$  s.e.m. ( $\log_2(\text{mRNA copies} + 1)$ ), *power* = 0. (f) Period gene 2 (*Per2*) mRNA localization by *in situ* hybridization in the SCN. (g) Neuromedin S (NMS) immunoreactivity around the third ventricle (3V) including synaptic boutons co-stained for the presynaptic protein VAMP2. The existence of particular neuronal subclasses was confirmed by *in situ* hybridization data from the open source Allen Brain Atlas database ([www.brain-map.org](http://www.brain-map.org)). Abbreviations: 3V, third ventricle. Scale bars = 150  $\mu\text{m}$  (a,b,c left,c<sub>1</sub>), 70  $\mu\text{m}$  (f left), 20  $\mu\text{m}$  (c right,f right).

Romanov, Zeisel *et al.* – Table 1

<b>Genes</b>	<b>Peptides</b>	<b>Molecule count</b>
Adcyap1	Adenylate-cyclase activating polypeptide 1 (Pituitary)	417
Agrp	Agouti-related neuropeptide	1,406
Avp	Arginine-vasopressin	14,529
Bdnf	Brain-derived neurotrophic factor	504
Calca	Calcitonin	55
Calcb	Calcitonin 2	8
Cartpt	Cocaine- and amphetamine-regulated transcript protein	4,833
Cck	Cholecystokinin	437
Cgrp	Calcitonin gene-related peptide	0
Cort	Cortistatin	0
Crh	Corticotropin-releasing hormone	886
Gal	Galanin	7,309
Ghrh	Growth hormone-releasing hormone	419
Ghrl	Ghrelin	0
Gnrh1	Gonadotropin-releasing hormone 1 (luteinizing-releasing hormone)	1,370
Grp	Gastrin-releasing peptide	110
Hcrt	Orexin (hypocretin)	10,682
Ins	Insulin	0
Insl5	Insulin-like peptide 5	33
Insl6	Insulin-like peptide 6	3
Lep	Leptin	0
Nmb	Neuromedin B	91
Nms	Neuromedin S	109
Nmu	Neuromedin U	16
Npb	Neuropeptide B	17
Npff	Neuropeptide FF-amide peptide	20
Nppa	Natriuretic Peptide A	11
Nppc	Natriuretic Peptide C	136
Npvf	Neuropeptide VF	2,617
Npw	Neuropeptide W	25
Npy	Neuropeptide Y	2,459
Nts	Neurotensin	1,565
Oxt	Oxytocin	31,901
Pdyn	$\beta$ -Neoendorphin, dynorphin, leu-enkephalin, rimorphin, leumorphin	68
Penk	Met- and Leu-enkephalin, adrenorphin, amidorphin	649
Pmch	Melanin-concentrating hormone	24,187
Pnoc	Nociceptin	682
Pomc	$\alpha$ -, $\beta$ - and $\gamma$ -MSH, $\beta$ -endorphin, ACTH, LPH, met-enkephalin	670
Ppy	Pancreatic polypeptide	0
Prok2	Prokineticin2	70
Pyy	Peptide YY	0
Qrfp	Pyroglutamylated RFamide peptide	194
Rln1	Relaxin	83
Rln2	Relaxin 2	0
Rln3	Relaxin 3	0
Spx	Neuropeptide Q	0
Sst	Somatostatin	32,234
Tac1	Substance P, neurokinin A, neuropeptide K, neuropeptide $\gamma$	2,208
Tac2	Neurokinin B, neuromedin K	765
Tac4	Tachykinin-4	7
Trh	Thyrotropin-releasing hormone	3,171
Ucn	Urocortin	0
Ucn2	Urocortin 2	0
Ucn3	Urocortin 3	20
Vip	Vasoactive intestinal peptide	670